INVESTIGATION OF THE BIOTRANSFORMATION OF ALC-0159 AND ALC-0315 IN VITRO AND IN VIVO IN RATS

LIST OF ABBREVIATIONS

Abbreviation	Term
ALC-0159	Proprietary PEG-lipid included as an excipient in the LNP formulation used in the COVID-19 mRNA vaccine
ALC-0315	Proprietary amino-lipid included as an excipient in the LNP formulation used in the COVID-19 mRNA vaccine
COVID-19	Coronavirus disease 2019
DMSO	Dimethyl sulfoxide
LNP	Lipid-nanoparticles
MeCN	Acetonitrile
modRNA	Nucleoside-modified mRNA
mRNA	Messenger RNA
NAD+	Nicotinamide adenine dinucleotide (oxidized form)
NADH	Nicotinamide adenine dinucleotide (reduced form)
NADP+	Nicotinamide adenine dinucleotide phosphate (oxidized form)
NADPH	Nicotinamide adenine dinucleotide phosphate (reduced form)
PAPS	3'-Phosphoadenosine-5'-phosphosulfate
PEG	Polyethylene glycol
S9	Supernatant obtained from liver homogenate by centrifuging at 9000g
UDPGA	Uridine diphosphate glucuronic acid
UHPLC	Ultra high-performance liquid chromatography

1. ABSTRACT

The metabolism of the novel excipients, ALC-0159 and ALC-0315, was examined *in vitro* using blood, liver S9 fractions and hepatocytes, all from mouse, rat, monkey and human. The *in vivo* metabolism was examined in rat plasma, urine, feces, and liver from a rat pharmacokinetics study where a luciferase-encoding mod RNA formulated in LNP with an identical lipid composition as PF-07302048 (COVID-19 mRNA Vaccine; BioNTech code number BNT162) was administered intravenously at a 1 mg/kg dose.

The primary route of metabolism identified for ALC-0159 involves amide bond hydrolysis yielding *N*,*N*-ditetradecylamine (*m/z* 410). This metabolite was identified in mouse and rat blood, as well as hepatocytes and liver S9 from mouse, rat, monkey and human. No metabolites of ALC-0159 were identified from *in vivo* samples.

Metabolism of ALC-0315 occurs via two sequential ester hydrolysis reactions, first yielding the monoester metabolite (*m/z* 528) followed by the doubly deesterified metabolite (*m/z* 290). The monoester metabolite was observed *in vitro* in rat blood, monkey S9 fraction, and *in vivo* in rat plasma and rat liver. The doubly deesterified metabolite was observed *in vitro* in mouse and rat blood; monkey liver S9 fraction; and *in vivo* in rat plasma, urine, feces and liver. Subsequent metabolism of the doubly deesterified metabolite resulted in a glucuronide metabolite (*m/z* 466) which was observed in urine only from the rat pharmacokinetics study. Additionally, 6-hexyldecanoic acid (*m/z* 255), the acid product of both ester hydrolysis reactions of ALC-0315, was identified *in vitro* in mouse and rat blood; mouse, rat, monkey and human hepatocytes; mouse, rat and human liver S9 fractions; and *in vivo* in rat plasma.

Based on nonquantitative ion current data for parent depletion and metabolite formation, metabolism for both ALC-0159 and ALC-0315 appears to occur relatively slowly across most species *in vitro* and *in vivo*. Overall, it can be concluded that both ALC-0159 and ALC-0315 are metabolized by hydrolytic metabolism of the amide or ester functionalities, respectively, and this hydrolytic metabolism is observed across the species evaluated.

2. OBJECTIVES

The objective of this study was to provide a preliminary qualitative assessment of the biotransformation of the novel excipients ALC-0159 and ALC-0315 in blood, liver S9 fractions and hepatocytes from mouse, rat, monkey and human as well as in plasma, urine, feces and liver samples from a rat pharmacokinetics study.

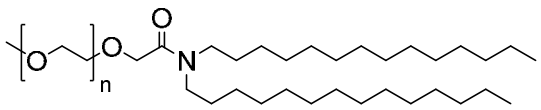

ALC-0159 (n = 40-51)
n = 45, major component

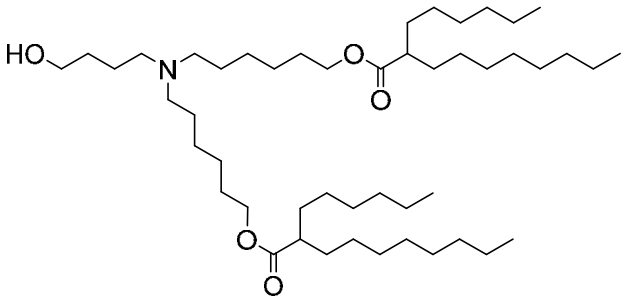

ALC-0315

3. MATERIALS AND METHODS

3.1. Materials

ALC-0159 (2-[(polyethylene glycol]-2000]-*N*,*N*-ditetradecylacetamide, Lot# GALC0159-10), ALC-0315 ((4-hydroxybutyl)azanediyl)bis(hexane-6,1-diyl) bis(2-hexyldecanoate), Lot# GALC0315-11), and Carboxy-MPEG2 (methoxypolyethylene glycol 2000 acetic acid, Lot# 792354-01-011) were obtained from Avanti Polar Lipids, Inc. NAD+, reduced NADH, reduced NADPH, NADP+, alamethicin, adipic acid, diethylene glycol, triethylene glycol, tetraethylene glycol, myristic acid, tetradecylamine, 6-hexyldecanoic acid, 4-aminobutyric acid, and 6-aminohexanoic acid were obtained from Millipore-Sigma (St. Louis, MO). *N*,*N*-Ditetradecylamine was obtained from Ambeed (Arlington Heights, IL). All other reagents were the highest grade commercially available.

Blood from mouse (female, CD-1), rat (male, Wistar Han), monkey (male, cynomolgus), and human (one male and one female) was obtained from in-house untreated animals and from human donors not taking any medications. Potassium EDTA (K_2EDTA) was used as the anticoagulant for all species. In all species except rat, the blood used for the *in vitro* assessments was a pool of 2 or more animals or donors. Mouse (male, CD-1, BioIVT, lot YKA), rat (male, Wistar Han, BioIVT, lot DTO), monkey (male, cynomolgus, BioIVT, lot DNB), and human (mixed gender, BioIVT, lot SPB) hepatocytes were used in the *in vitro* assessments. Mouse liver S9 fraction (Xenotech, female, CD-1, lot# 0310217, 20 mg/mL protein), rat liver S9 fraction (BD Gentest, male Wistar Han, lot# 58237, 20 mg/mL protein), monkey liver S9 (Xenotech, male, cynomolgus, lot# 0210398, 20 mg/mL) and human liver S9 (Celsis, Lot ABT, 20 mg/mL protein) were utilized for the *in vitro* assessments.

3.2. Blood

Mouse, rat, monkey and human blood were spiked with ALC-0159 and ALC-0315 stock solutions (1 mM, each dissolved in DMSO) to give a final concentration of 10 μM. A solvent control was also included where DMSO was added in place of test compound. After addition of test compound or DMSO, blood samples were maintained at 37 °C. Aliquots (500 μL) were removed at 0, 0.5, 1, 2, 4, 6, and 24 h and quenched with 6 volumes of ice-cold MeCN. Samples were subsequently centrifuged at 1860 x g for 5 minutes. The samples were then transferred to clean 15 mL glass tubes and evaporated to dryness using a Genevac evaporative centrifuge. To expedite analyses, only the 0 and 24 h samples were reconstituted

in 100 µL of 1% MeCN in water and analyzed as described below. The remaining samples were stored at -40 °C.

3.3. Hepatocytes

Mouse, rat, monkey and human hepatocyte incubations (0.75 x 10^6 cells/mL), were conducted at a final concentration of ALC-0159 and ALC-0315 of 10 µM using 1 mM stocks, each dissolved in DMSO. A solvent control was also included where DMSO was added in place of test compound. After addition of test compound or DMSO, samples were maintained in an incubator at 37 °C, 95% humidity, and 5% carbon dioxide. Aliquots (500 µL) were removed at 0, 0.5, 1, 2, and 3 h and a 250 µL at 4 h and quenched with 6 volumes of ice-cold MeCN. Samples were subsequently centrifuged at 1860 x g for 5 minutes. The samples were then transferred to clean 15 mL glass tubes and evaporated to dryness using a Genevac evaporative centrifuge. To expedite analyses, only the 0 and 4 h samples were analyzed. The 0 h samples were reconstituted in 100 µL of 1% MeCN in water and 4 h samples in 50 µL of 1% MeCN in water and analyzed as described below. The remaining samples were stored at -40 °C.

3.4. Liver S9 Fractions

Liver S9 fractions from mouse, rat, monkey, and human suspended in 0.1 M phosphate buffer (pH 7.4) containing 3.3 mM magnesium chloride were preincubated with alamethicin (9 µg/mL) for 15 min on ice. Incubations were started by addition of a mixture of test compound dissolved in DMSO and buffer, test compound dissolved in DMSO, buffer, and cofactor mix A (1 mM NADPH, 1 mM NADH, 0.5 mM PAPS, and 2.5 mM UDPGA), or test compound, buffer and cofactor mix B (1 mM NADP+, 1 mM NAD+, 0.5 mM PAPS, and 2.5 mM UDPGA), bringing the incubation to a total volume of 1 mL with a final protein concentration of 1 mg/mL and a final concentration of ALC-0159 or ALC-0315 of 10 µM. Incubation mixtures were warmed to 37 °C, and aliquots (150 µL) were removed at 0, 0.5, 1, 2, 4, 6, and 24 h and quenched by addition to MeCN (400 µL). Samples were subsequently centrifuged at 3000 rpm (1860 x g) for 5 minutes. The samples were then transferred to clean 1 mL glass dolphin-nosed tubes and evaporated to dryness using a Genevac evaporative centrifuge. To expedite analyses, only the 0 and 24 h samples were reconstituted in 100 µL of 1% MeCN in water and analyzed as described below. The remaining samples were stored at -40 °C.

3.5. Rat Pharmacokinetics Study Samples

Plasma, urine, feces and liver samples were obtained from a 14-day rat pharmacokinetics study (Study PF-07302048_06Jul20_072424[1]) where a luciferase-encoding mod RNA formulated in LNP with an identical lipid composition as PF-07302048 (COVID-19 mRNA Vaccine; BioNTech code number BNT162) was administered intravenously at a 1 mg/kg mod RNA dose to male, Wistar Han rats. At this mod RNA dose, the dose of ALC-0159 was 1.96 mg/kg and of ALC-0315 was 15.3 mg/kg. While additional time point samples were obtained of pharmacokinetic analysis, for metabolite identification studies, plasma and livers from three rats per time point at the following time points were used: pre-dose, 0.1, 24, 96, 192, and 336 h post-dose. Fecal and urine samples from three rats per time point from pre-dose, 0-24, 24-48, 72-96, 168-192, and 312-336 h post-dose were used.

3.5.1. Plasma Sample Preparation

Plasma (50 µL) from each rat per time point was pooled to generate pools for the pre-dose, 0.1, 24, 96, 192, and 336 h time points. Proteins were precipitated with 4 volumes of ice-cold MeCN, centrifuged, and the supernatant blown to dryness. Residues were reconstituted in 100 µL of 1% MeCN in water and analyzed as described below.

3.5.2. Urine Sample Preparation

Urine samples (100 µL from each rat) for the pre-dose, 0-24, 24-48, 72-96, 168-192, and 312-336 h time points were combined to generate a sample pool for each of these time points. Pooled urine samples were centrifuged at 17000 x g for 10 minutes. Supernatants were transferred to analyses tubes and analyzed without further manipulation and analyzed as described below.

3.5.3. Feces Sample Preparation

Feces samples for each rat fecal sample from the pre-dose, 0-24, 24-48, 72-96, 168-192, and 312-336 h time points were diluted 1:9 (w/v) with homogenization solution (60:40 isopropyl alcohol/water) and homogenized with a Mini-Beadbeater-96 (BioSpec Products) using 2 mm zirconia beads and a 2 minute homogenization time. Homogenized samples (300 µL) for the three rat samples per time point were pooled. Proteins were precipitated with 4 volumes of ice-cold MeCN, centrifuged, and the supernatant blown to dryness. Residues were reconstituted in 100 µL of 1% MeCN in water and analyzed as described below.

3.5.4. Liver Sample Preparation

Liver samples for each rat from the pre-dose, 0.1, 24, 96, 192, and 336 h time points were diluted 1:4 (w/v) with homogenization solution (60:40 isopropyl alcohol/water) and homogenized with a Mini-Beadbeater-96 (BioSpec Products) using 2 mm zirconia beads and a 2 minute homogenization time. Homogenized samples (200 µL) for the three rat samples per time point were pooled. Proteins were precipitated with 4 volumes of ice-cold MeCN, centrifuged, and the supernatant blown to dryness. Residues were reconstituted in 100 µL of 1% MeCN in water and analyzed as described below.

3.6. UHPLC-MS/MS Analysis

3.6.1. UHPLC-MS/MS Sample Analysis of ALC-0159

Reconstituted samples were analyzed using the same UHPLC method but with separate MS/MS analyses in positive ion and negative ion electrospray modes using a Thermo Orbitrap Elite mass spectrometer. Xcalibur software version 3.0.63 was used to control the UHPLC-MS system. Injections of 2 µL were made by a CTC PAL autosampler. Full scan data were collected at 15,000 resolution. The UHPLC system consisted of an Accela quaternary solvent delivery pump (Thermo Electron Corporation). An Acquity UPLC C8 100 Å column was used (2.1 x 100 mm, 1.7 µm) with a flow rate of 0.4 mL/min heated to 45 °C in a Hot Sleeve column heater (Analytical Sales and Services). Mobile phase A was 10 mM ammonium acetate buffer (pH 4.5) and mobile phase B was MeCN.

Time, min	%A	%B	Flow Rate (µL/min)
0.0	100	0	400
2.5	100	0	400
5.0	40	60	400
23.0	5	95	400
26.0	5	95	400
26.1	100	0	400
30.0	100	0	400

3.6.2. UHPLC-MS/MS Sample Analysis of ALC-0315

Reconstituted samples were analyzed using the same UHPLC method but with separate MS/MS analyses in positive ion and negative ion electrospray modes using a Thermo Orbitrap Elite mass spectrometer. Xcalibur software version 3.0.63 was used to control the UHPLC-MS system. Injections of 5 µL were made by a CTC PAL autosampler. Full scan data were collected at 15,000 resolution. The UHPLC system consisted of an Accela quaternary solvent delivery pump (Thermo Electron Corporation). An Acquity UPLC C18 100 Å column was used (2.1 x 150 mm, 1.7 µm) with a flow rate of 0.3 mL/min heated to 45 °C in a Hot Sleeve column heater (Analytical Sales and Services). Mobile phase A was 0.1 % formic acid in water and mobile phase B was MeCN.

Time, min	%A	%B	Flow Rate (µL/min)
0.0	100	0	300
2.5	100	0	300
5.0	90	10	300
10.0	50	50	300
17.5	5	95	300
21.5	5	95	300
21.6	100	0	300
25.0	100	0	300

4. RESULTS & DISCUSSION

As shown in Figure 9.1, the primary route of metabolism identified for ALC-0159 involves amide bond hydrolysis yielding *N*,*N*-ditetradecylamine (*m/z* 410). This metabolite was identified in mouse and rat blood as well as hepatocytes and liver S9 from mouse, rat, monkey and human. Theoretical metabolites were arrived at via examination of the excipient molecules and consideration of commonly observed biotransformations (hydroxylation, *N*-dealkylation, hydrolysis, glucuronidation, sulfation, oxidation and combinations thereof). Summaries of the masses of theoretical and observed metabolites of ALC-0159 for blood, hepatocytes, liver S9 fractions, and rat pharmacokinetics samples are presented in Tables 8.1, 8.2, 8.3, and 8.4, respectively. Representative example chromatograms from *in vitro* incubations of ALC-0159 with mouse hepatocytes, human hepatocytes, and *in vivo* samples from a rat pharmacokinetics study are presented in Figures 9.3, 9.4, and 9.5, respectively. No metabolites of ALC-0159 were identified from *in vivo* samples.

Metabolism of ALC-0315 occurs via two sequential ester hydrolysis reactions, first yielding the monoester metabolite (*m/z* 528) followed by the doubly deesterified metabolite (*m/z* 290) as shown in Figure 9.2. The monoester metabolite was observed in vitro in rat blood, monkey S9 fraction, and *in vivo* in rat plasma and rat liver. The doubly deesterified metabolite was observed *in vitro* in mouse and rat blood; monkey liver S9 fraction; and *in vivo* in rat plasma, urine, feces and liver. Subsequent metabolism of the doubly desterified metabolite resulted in a glucuronide metabolite (*m/z* 466) which was observed in urine only from the rat pharmacokinetics study. Additionally, 6-hexyldecanoic acid (*m/z* 255), the acid product of both hydrolysis reactions of ALC-0315, was identified *in vitro* in mouse and rat blood; mouse, rat, monkey and human hepatocytes; mouse, rat and human liver S9 fractions; and *in vivo* in rat plasma. Summaries of the masses of theoretical and observed metabolites of ALC-0315 for blood, hepatocytes, liver S9 fractions, and rat pharmacokinetics samples are presented in Tables 8.5, 8.6, 8.7, and 8.8, respectively. Representative example chromatograms from *in vitro* incubations of ALC-03159 with monkey liver S9 fraction, human hepatocytes, and *in vivo* samples from a rat pharmacokinetics study are presented in Figures 9.6, 9.7, and 9.8, respectively.

Based on nonquantitative ion current data for parent depletion and metabolite formation, metabolism for both ALC-0159 and ALC-0315 appears to occur relatively slowly across most species *in vitro* and *in vivo*. Overall, it can be concluded that both ALC-0159 and ALC-0315 are metabolized by hydrolytic metabolism of the amide or ester functionalities, respectively, and this hydrolytic metabolism is observed across the species evaluated.

4.1. Mass Spectral Analysis of ALC-0159

Mass spectrometric analyses of ALC-0159 indicate that it is a mixture of varying polyethylene glycol (PEG) lengths ranging between approximately 40-51 ethylene glycol units. Additionally, the mass spectrum (Figure 9.9) indicates that this mixture of compounds also exists in +2, +3, and +4 charge states with the +4 charge state being the most abundant. Deconvolution of the most abundant ion in the +4 charge state (*m/z* 629.6939, t_R = 19.1 minutes) is consistent with a triply ammoniated, protonated species. For simplicity of analyses and description, PEG-containing metabolites of ALC-0159, where standards are not available, were searched for based on modifications of the most abundant and intense parent mass (*m/z* 629.6939).

4.2. Mass Spectral Analysis of ALC-0159 *m/z* 410 metabolite

An *m/z* 410 metabolite of ALC-0159 had a retention time of approximately 16.9 minutes with a protonated molecular ion of *m/z* 410.4715. It was observed in mouse and rat blood, as well as hepatocytes and liver S9 from mouse, rat, monkey and human. The product ion spectrum for *m/z* 410 possessed a single fragment ion of *m/z* 214 which corresponds to loss of one of the 14-carbon aliphatic chains. Both the observed retention time and fragmentation pattern for *m/z* 410 match those obtained from *N*,*N*-ditetradecylamine (Figure 9.10)

4.3. Mass Spectral Analysis of ALC-0315

ALC-0315 was identified at a retention time of 20.0 minutes and *m/z* 766.7254. Product ion spectrum fragment ions at *m/z* 748, 694 and 510 were observed in as shown in Figure 9.11. The *m/z* 748 fragment is consistent with a water loss from butyl alcohol substituent. The *m/z*

694 fragment corresponds to loss of the butyl alcohol substituent. The *m/z* 272 fragment is consistent with loss of one of the 6-hexyldecanoic acid moieties along with H+.

4.4. Mass Spectral Analysis of ALC-0315 *m/z* 528 Metabolite

A metabolite of ALC-0315 with a retention time of 15.9 minutes and *m/z* 528.4975. This metabolite was observed in rat blood, monkey liver S9 fraction, rat plasma and rat liver samples. Product ion spectrum fragment ions at *m/z* 510, 456, 272 and 218 were observed as shown in Figure 9.12. The *m/z* 510 fragment is consistent with a water loss from one of the two alkyl alcohol substituents. The *m/z* 456 fragment corresponds to loss of the butyl alcohol substituent. The *m/z* 272 fragment is consistent with loss of the 6-hexyldecanoic acid moiety along with H+.

4.5. Mass Spectral Analysis of ALC-0315 *m/z* 290 Metabolite

A metabolite of ALC-0315 was observed at 8.0 minutes with *m/z* 290.2688. This metabolite was observed in mouse and rat blood, monkey liver S9 fraction, and plasma, urine, feces and liver from the rat pharmacokinetics study. The product ion spectrum displays fragment ions of *m/z* 272 (loss of water) and *m/z* 218 (loss of butyl alcohol substituent) (Figure 9.13).

4.6. Mass Spectral Analysis of ALC-0315 *m/z* 466 Metabolite

The *m/z* 466 metabolite of ALC-0315 was observed at 7.9 minutes with *m/z* 466.3006 only in rat urine. The product ion spectra of shows a single fragment with *m/z* 290 (Figure 9.14). A neutral loss of 176 Da for this metabolite is consistent with a glucuronide conjugate to one of the three alcohol moieties of the doubly deesterified metabolite, *m/z* 290.

4.7. Mass Spectral Analysis of ALC-0315 *m/z* 255 Metabolite

An *m/z* 255 metabolite of ALC-0315 was observed at approximately 19.7 min with *m/z* 255.2324 in mouse plasma. This metabolite was observed in mouse and rat blood; mouse, rat, monkey and human hepatocytes; mouse, rat and human liver S9 fractions; and *in vivo* in rat plasma. This metabolite matches by both retention time and exact mass with a synthetic standard of 6-hexyldecanoic acid. However, product ion spectra could not be obtained for either the metabolite or the 6-hexyldecanoic acid standard.

5. CONCLUSIONS

The metabolism of the novel excipients, ALC-0159 and ALC-0315, were examined *in vitro* using blood, liver S9 fractions and hepatocytes, all from mouse, rat, monkey and human. The *in vivo* metabolism was examined in rat plasma, urine, feces, and liver from a rat pharmacokinetics study where a luciferase-encoding mod RNA formulated in an LNP with an identical lipid composition as PF-07302048 was administered intravenously at a 1 mg/kg dose.

The primary route of metabolism identified for ALC-0159 involves amide bond hydrolysis yielding *N*,*N*-ditetradecylamine (*m/z* 410). This metabolite was identified in mouse and rat blood, as well as hepatocytes and liver S9 from mouse, rat, monkey and human. No metabolites of ALC-0159 were identified from *in vivo* samples.

Metabolism of ALC-0315 occurs via two sequential ester hydrolysis reactions, first yielding the monoester metabolite (*m/z* 528) followed by the doubly deesterified metabolite (*m/z* 290). The monoester metabolite was observed *in vitro* in rat blood, monkey S9 fraction, and *in vivo* in rat plasma and rat liver. The doubly deesterified metabolite was observed *in vitro* in mouse and rat blood; monkey liver S9 fraction; and *in vivo* in rat plasma, urine, feces and liver. Subsequent metabolism of the doubly deesterified metabolite resulted in a glucuronide metabolite (*m/z* 466) which was observed in urine only from the rat pharmacokinetics study. Additionally, 6-hexyldecanoic acid (*m/z* 255), the acid product of both hydrolysis reactions of ALC-0315, was identified *in vitro* in mouse and rat blood; mouse, rat, monkey and human hepatocytes; mouse, rat and human liver S9 fractions; and *in vivo* in rat plasma.

Based on nonquantitative ion current data for parent depletion and metabolite formation, metabolism for both ALC-0159 and ALC-0315 appears to occur relatively slowly across most species *in vitro* and *in vivo*. Overall, it can be concluded that both ALC-0159 and ALC-0315 are metabolized by hydrolytic metabolism of the amide or ester functionalities, respectively, and this hydrolytic metabolism is observed across the species evaluated.

6. ARCHIVING

Data presented in this report can be found in the following locations:

Laboratory Notebooks	/Root/PDM/Groton/ (b) (6) VBN#00710777/COVID_Excipient/200715_COVID_Novel_Excipients_HHEP /Root/PDM/Groton/ (b) (6) VBN#00710777/COVID_Excipient/200728_COVID_Novel_Excipients_Blood_Stability /Root/PDM/Groton/ (b) (6) VBN#00710777/COVID_Excipient/200728_COVID_Novel_Excipients_S9 /Root/PDM/Groton/ (b) (6) VBN#00710777/COVID_Excipient/200820_COVID_excipient_rat_PK_met_ID

Laboratory Notebooks	/Root/PDM/Groton/ (b) (6) VBN#00710777/COVID_Excipient/200715_COVID_Novel_Excipients_HHEP /Root/PDM/Groton/ (b) (6) VBN#00710777/COVID_Excipient/200728_COVID_Novel_Excipients_Blood_Stability /Root/PDM/Groton/ (b) (6) VBN#00710777/COVID_Excipient/200728_COVID_Novel_Excipients_S9 /Root/PDM/Groton/ (b) (6) VBN#00710777/COVID_Excipient/200820_COVID_excipient_rat_PK_met_ID
Analytical Archive Reference	Open Lab: Enterprise/Content/Target Archive/ COVID vaccine excipients/Biotransformation/ 200730_COVID_Excipient_HEP Enterprise/Content/Target Archive/ COVID vaccine excipients/Biotransformation/ 200730_COVID_Excipients_LS9 Enterprise/Content/Target Archive/ COVID vaccine excipients/Biotransformation/ 200731_COVID_Excipient_Blood Enterprise/Content/Target Archive/ COVID vaccine excipients/Biotransformation/ 200822_COVID_Excipient_Rat_PK

7. REFERENCES

1. PF-07302048_06Jul20_072424_A single dose pharmacokinetics study of ALC-0315 and ALC-0159 following intravenous bolus injection of PF-07302048 Nanoparticle Formulation in Wistar Han Rats. 01 Sept 2020.

8. SUPPORTIVE TABLES

8.1. *In Vitro* Assessment of ALC-0159 Metabolites in Mouse, Rat, Monkey and Human Blood

m/z	Biotransformation	t_R, min	Blood			
			Mouse	Rat	Monkey	Human
107.0703[b]	*O*-Demethylation, *O*-dealkylation	1.2[c]	ND	ND	ND	ND
151.0965[b]	*O*-Demethylation, *O*-dealkylation	3.1[c]	ND	ND	ND	ND
195.1227[b]	*O*-Demethylation, *O*-dealkylation	4.8[c]	ND	ND	ND	ND
214.2529[b]	Hydrolysis, *N*-dealkylation	7.3[c]	ND	ND	ND	ND
227.2017[a]	*N*-Dealkylation, oxidation	9.1[c]	ND	ND	ND	ND
410.4720[b]	Hydrolysis (amine)	16.9[c]	+	+	ND	ND
531.5849[b]	*N*,*N*-Didealkylation	ND	ND	ND	ND	ND
580.6396[b]	*N*-Dealkylation	ND	ND	ND	ND	ND
629.6853[b]	*O*-Demethylation, oxidation	ND	ND	ND	ND	ND
633.6931[b]	Hydroxylation	ND	ND	ND	ND	ND
637.1880[b]	ω-Hydroxylation, oxidation	ND	ND	ND	ND	ND
708.7721[b]	Hydrolysis (acid)	5.8[c]	ND	ND	ND	ND

a. Negative ion mode
b. Positive ion mode
c. Determined using standard
ND – Not Detected, + = metabolite identified.

8.2. *In Vitro* Assessment of ALC-0159 Metabolites in Mouse, Rat, Monkey and Human Hepatocytes

m/z	Biotransformation	t_R, min	Hepatocytes			
			Mouse	Rat	Monkey	Human
107.0703[b]	*O*-Demethylation, *O*-dealkylation	1.2[c]	ND	ND	ND	ND
151.0965[b]	*O*-Demethylation, *O*-dealkylation	3.1[c]	ND	ND	ND	ND
195.1227[b]	*O*-Demethylation, *O*-dealkylation	4.8[c]	ND	ND	ND	ND
214.2529[b]	Hydrolysis, *N*-dealkylation	7.3[c]	ND	ND	ND	ND
227.2017[a]	*N*-Dealkylation, oxidation	9.1[c]	ND	ND	ND	ND
410.4720[b]	Hydrolysis (amine)	16.9[c]	+	+	+	+
531.5849[b]	*N*,*N*-Didealkylation	ND	ND	ND	ND	ND
580.6396[b]	*N*-Dealkylation	ND	ND	ND	ND	ND
629.6853[b]	*O*-Demethylation, oxidation	ND	ND	ND	ND	ND
633.6931[b]	Hydroxylation	ND	ND	ND	ND	ND
637.1880[b]	ω-Hydroxylation, oxidation	ND	ND	ND	ND	ND
708.7721[b]	Hydrolysis (acid)	5.8[c]	ND	ND	ND	ND

a. Negative ion mode
b. Positive ion mode
c. Determined using standard
ND – Not Detected, + = metabolite identified.

8.3. *In Vitro* Assessment of ALC-0159 Metabolites in Mouse, Rat, Monkey and Human Liver S9 Fractions

m/z	Biotransformation	t_R, min	Liver S9 Fractions			
			Mouse	Rat	Monkey	Human
107.0703[b]	*O*-Demethylation, *O*-dealkylation	1.2[c]	ND	ND	ND	ND
151.0965[b]	*O*-Demethylation, *O*-dealkylation	3.1[c]	ND	ND	ND	ND
195.1227[b]	*O*-Demethylation, *O*-dealkylation	4.8[c]	ND	ND	ND	ND
214.2529[b]	Hydrolysis, *N*-dealkylation	7.3[c]	ND	ND	ND	ND
227.2017[a]	*N*-Dealkylation, oxidation	9.1[c]	ND	ND	ND	ND
410.4720[b]	Hydrolysis (amine)	16.9[c]	+	+	+	+
531.5849[b]	*N*,*N*-Didealkylation	ND	ND	ND	ND	ND
580.6396[b]	*N*-Dealkylation	ND	ND	ND	ND	ND
629.6853[b]	*O*-Demethylation, oxidation	ND	ND	ND	ND	ND
633.6931[b]	Hydroxylation	ND	ND	ND	ND	ND
637.1880[b]	ω-Hydroxylation, oxidation	ND	ND	ND	ND	ND
708.7721[b]	Hydrolysis (acid)	5.8[c]	ND	ND	ND	ND

a. Negative ion mode
b. Positive ion mode
c. Determined using standard
ND – Not Detected, + = metabolite identified.

8.4. Assessment of Metabolites of ALC-0159 in Plasma, Urine, Feces, and Liver from a Rat Pharmacokinetics Study.

m/z	Biotransformation	t_R, min	Rat *In Vivo*			
			Plasma	Urine	Feces	Liver
107.0703[b]	*O*-Demethylation, *O*-dealkylation	1.2[c]	ND	ND	ND	ND
151.0965[b]	*O*-Demethylation, *O*-dealkylation	3.1[c]	ND	ND	ND	ND
195.1227[b]	*O*-Demethylation, *O*-dealkylation	4.8[c]	ND	ND	ND	ND
214.2529[b]	Hydrolysis, *N*-dealkylation	7.3[c]	ND	ND	ND	ND
227.2017[a]	*N*-Dealkylation, oxidation	9.1[c]	ND	ND	ND	ND
410.4720[b]	Hydrolysis (amine)	16.9[c]	ND	ND	ND	ND
531.5849[b]	*N*,*N*-Didealkylation	ND	ND	ND	ND	ND
580.6396[b]	*N*-Dealkylation	ND	ND	ND	ND	ND
629.6853[b]	*O*-Demethylation, oxidation	ND	ND	ND	ND	ND
633.6931[b]	Hydroxylation	ND	ND	ND	ND	ND
637.1880[b]	ω-Hydroxylation, oxidation	ND	ND	ND	ND	ND
708.7721[b]	Hydrolysis (acid)	5.8[c]	ND	ND	ND	ND

a. Negative ion mode
b. Positive ion mode
c. Determined using standard
ND – Not Detected, + = metabolite identified.

8.5. *In Vitro* Assessment of ALC-0315 Metabolites in Mouse, Rat, Monkey and Human Blood

m/z	Biotransformation	t_R, min	Blood			
			Mouse	Rat	Monkey	Human
102.0561[a]	*N*-Dealkylation, oxidation	ND	ND	ND	ND	ND
104.0706[b]	*N*-Dealkylation, oxidation	1.2[c]	ND	ND	ND	ND
130.0874[a]	*N*-Dealkylation, oxidation	ND	ND	ND	ND	ND
132.1019[b]	*N*-Dealkylation, oxidation	1.9[c]	ND	ND	ND	ND
145.0506[a]	*N*-Dealkylation, hydrolysis, oxidation	7.7[c]	ND	ND	ND	ND
255.2330[a]	Hydrolysis (acid)	19.7[c]	+	+	ND	ND
271.2279[a]	Hydrolysis, hydroxylation	ND	ND	ND	ND	ND
290.2690[b]	Bis-hydrolysis (amine)	8.1	+	+	ND	ND
431.2650[a]	Hydrolysis, glucuronidation	ND	ND	ND	ND	ND
464.2865[a]	Bis-hydrolysis (amine), glucuronidation	ND	ND	ND	ND	ND
466.3011[b]	Bis-hydrolysis (amine), glucuronidation	7.9	ND	ND	ND	ND
528.4986[b]	Hydrolysis (amine)	15.9	ND	+	ND	ND
704.5307[b]	Hydrolysis (amine), glucuronidation	ND	ND	ND	ND	ND
778.6930[a]	Oxidation to acid	ND	ND	ND	ND	ND
780.7076[b]	Oxidation to acid	ND	ND	ND	ND	ND
782.7232[b]	Hydroxylation	ND	ND	ND	ND	ND
844.6706[a]	Sulfation	ND	ND	ND	ND	ND
846.6851[b]	Sulfation	ND	ND	ND	ND	ND
940.7458[a]	Glucuronidation	ND	ND	ND	ND	ND
942.7604[b]	Glucuronidation	ND	ND	ND	ND	ND

a. Negative ion mode
b. Positive ion mode
c. Determined using standard
ND – Not Detected, + = metabolite identified.

8.6. *In Vitro* Assessment of ALC-0315 Metabolites in Mouse, Rat, Monkey and Human Hepatocytes

m/z	Biotransformation	t_R, min	Hepatocytes			
			Mouse	Rat	Monkey	Human
102.0561[a]	*N*-Dealkylation, oxidation	ND	ND	ND	ND	ND
104.0706[b]	*N*-Dealkylation, oxidation	1.2[c]	ND	ND	ND	ND
130.0874[a]	*N*-Dealkylation, oxidation	ND	ND	ND	ND	ND
132.1019[b]	*N*-Dealkylation, oxidation	1.9[c]	ND	ND	ND	ND
145.0506[a]	*N*-Dealkylation, hydrolysis, oxidation	7.7[c]	ND	ND	ND	ND
255.2330[a]	Hydrolysis (acid)	19.7[c]	+	+	+	+
271.2279[a]	Hydrolysis, hydroxylation	ND	ND	ND	ND	ND
290.2690[b]	Bis-hydrolysis (amine)	8.1	ND	ND	ND	ND
431.2650[a]	Hydrolysis, glucuronidation	ND	ND	ND	ND	ND
464.2865[a]	Bis-hydrolysis (amine), glucuronidation	ND	ND	ND	ND	ND
466.3011[b]	Bis-hydrolysis (amine), glucuronidation	7.9	ND	ND	ND	ND
528.4986[b]	Hydrolysis (amine)	15.9	ND	ND	ND	ND
704.5307[b]	Hydrolysis (amine), glucuronidation	ND	ND	ND	ND	ND
778.6930[a]	Oxidation to acid	ND	ND	ND	ND	ND
780.7076[b]	Oxidation to acid	ND	ND	ND	ND	ND
782.7232[b]	Hydroxylation	ND	ND	ND	ND	ND
844.6706[a]	Sulfation	ND	ND	ND	ND	ND
846.6851[b]	Sulfation	ND	ND	ND	ND	ND
940.7458[a]	Glucuronidation	ND	ND	ND	ND	ND
942.7604[b]	Glucuronidation	ND	ND	ND	ND	ND

a. Negative ion mode
b. Positive ion mode
c. Determined using standard
ND – Not Detected, + = metabolite identified.

8.7. *In Vitro* Assessment of ALC-0315 Metabolites in Mouse, Rat, Monkey and Human Liver S9 Fractions

m/z	Biotransformation	t_R, min	Liver S9 Fractions			
			Mouse	Rat	Monkey	Human
102.0561[a]	*N*-Dealkylation, oxidation	ND	ND	ND	ND	ND
104.0706[b]	*N*-Dealkylation, oxidation	1.2[c]	ND	ND	ND	ND
130.0874[a]	*N*-Dealkylation, oxidation	ND	ND	ND	ND	ND
132.1019[b]	*N*-Dealkylation, oxidation	1.9[c]	ND	ND	ND	ND
145.0506[a]	*N*-Dealkylation, hydrolysis, oxidation	7.7[c]	ND	ND	ND	ND
255.2330[a]	Hydrolysis (acid)	19.7[c]	+	+	ND	+
271.2279[a]	Hydrolysis, hydroxylation	ND	ND	ND	ND	ND
290.2690[b]	Bis-hydrolysis (amine)	8.1	ND	ND	+	ND
431.2650[a]	Hydrolysis, glucuronidation	ND	ND	ND	ND	ND
464.2865[a]	Bis-hydrolysis (amine), glucuronidation	ND	ND	ND	ND	ND
466.3011[b]	Bis-hydrolysis (amine), glucuronidation	7.9	ND	ND	ND	ND
528.4986[b]	Hydrolysis (amine)	15.9	ND	ND	+	ND
704.5307[b]	Hydrolysis (amine), glucuronidation	ND	ND	ND	ND	ND
778.6930[a]	Oxidation to acid	ND	ND	ND	ND	ND
780.7076[b]	Oxidation to acid	ND	ND	ND	ND	ND
782.7232[b]	Hydroxylation	ND	ND	ND	ND	ND
844.6706[a]	Sulfation	ND	ND	ND	ND	ND
846.6851[b]	Sulfation	ND	ND	ND	ND	ND
940.7458[a]	Glucuronidation	ND	ND	ND	ND	ND
942.7604[b]	Glucuronidation	ND	ND	ND	ND	ND

a. Negative ion mode
b. Positive ion mode
c. Determined using standard
ND – Not Detected, + = metabolite identified.

8.8. Assessment of Metabolites of ALC-0315 in Plasma, Urine, Feces, and Liver from a Rat Pharmacokinetics Study.

m/z	Biotransformation	t_R, min	Rat			
			Plasma	Urine	Feces	Liver
102.0561[a]	*N*-Dealkylation, oxidation	ND	ND	ND	ND	ND
104.0706[b]	*N*-Dealkylation, oxidation	1.2[c]	ND	ND	ND	ND
130.0874[a]	*N*-Dealkylation, oxidation	ND	ND	ND	ND	ND
132.1019[b]	*N*-Dealkylation, oxidation	1.9[c]	ND	ND	ND	ND
145.0506[a]	*N*-Dealkylation, hydrolysis, oxidation	7.7[c]	ND	ND	ND	ND
255.2330[a]	Hydrolysis (acid)	19.7[c]	+	ND	ND	ND
271.2279[a]	Hydrolysis, hydroxylation	ND	ND	ND	ND	ND
290.2690[b]	Bis-hydrolysis (amine)	8.1	+	+	+	+
431.2650[a]	Hydrolysis, glucuronidation	ND	ND	ND	ND	ND
464.2865[a]	Bis-hydrolysis (amine), glucuronidation	ND	ND	ND	ND	ND
466.3011[b]	Bis-hydrolysis (amine), glucuronidation	7.9	ND	+	ND	ND
528.4986[b]	Hydrolysis (amine)	15.9	+	ND	ND	+
704.5307[b]	Hydrolysis (amine), glucuronidation	ND	ND	ND	ND	ND
778.6930[a]	Oxidation to acid	ND	ND	ND	ND	ND
780.7076[b]	Oxidation to acid	ND	ND	ND	ND	ND
782.7232[b]	Hydroxylation	ND	ND	ND	ND	ND
844.6706[a]	Sulfation	ND	ND	ND	ND	ND
846.6851[b]	Sulfation	ND	ND	ND	ND	ND
940.7458[a]	Glucuronidation	ND	ND	ND	ND	ND
942.7604[b]	Glucuronidation	ND	ND	ND	ND	ND

a. Negative ion mode
b. Positive ion mode
c. Determined using standard
ND – Not Detected, + = metabolite identified.

9. SUPPORTIVE FIGURES

9.1. Proposed Biotransformation Pathway of ALC-0159 in Mouse (Mo), Rat (R), Monkey (Mk) and Human (H)

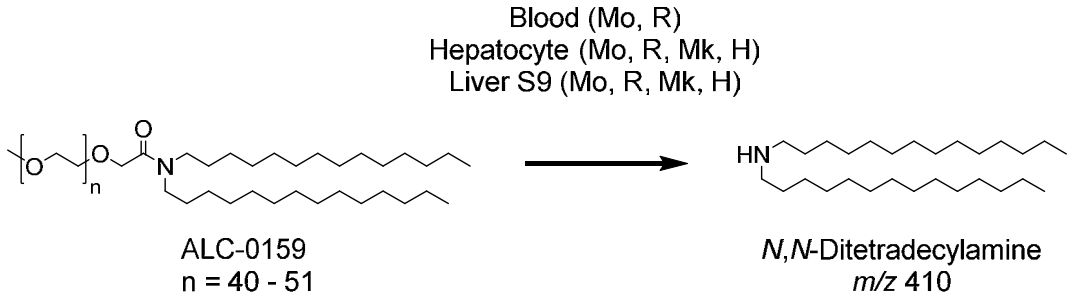

9.2. Proposed Biotransformation Pathway of ALC-0315 in Mouse (Mo), Rat (R), Monkey (Mk) and Human (H)

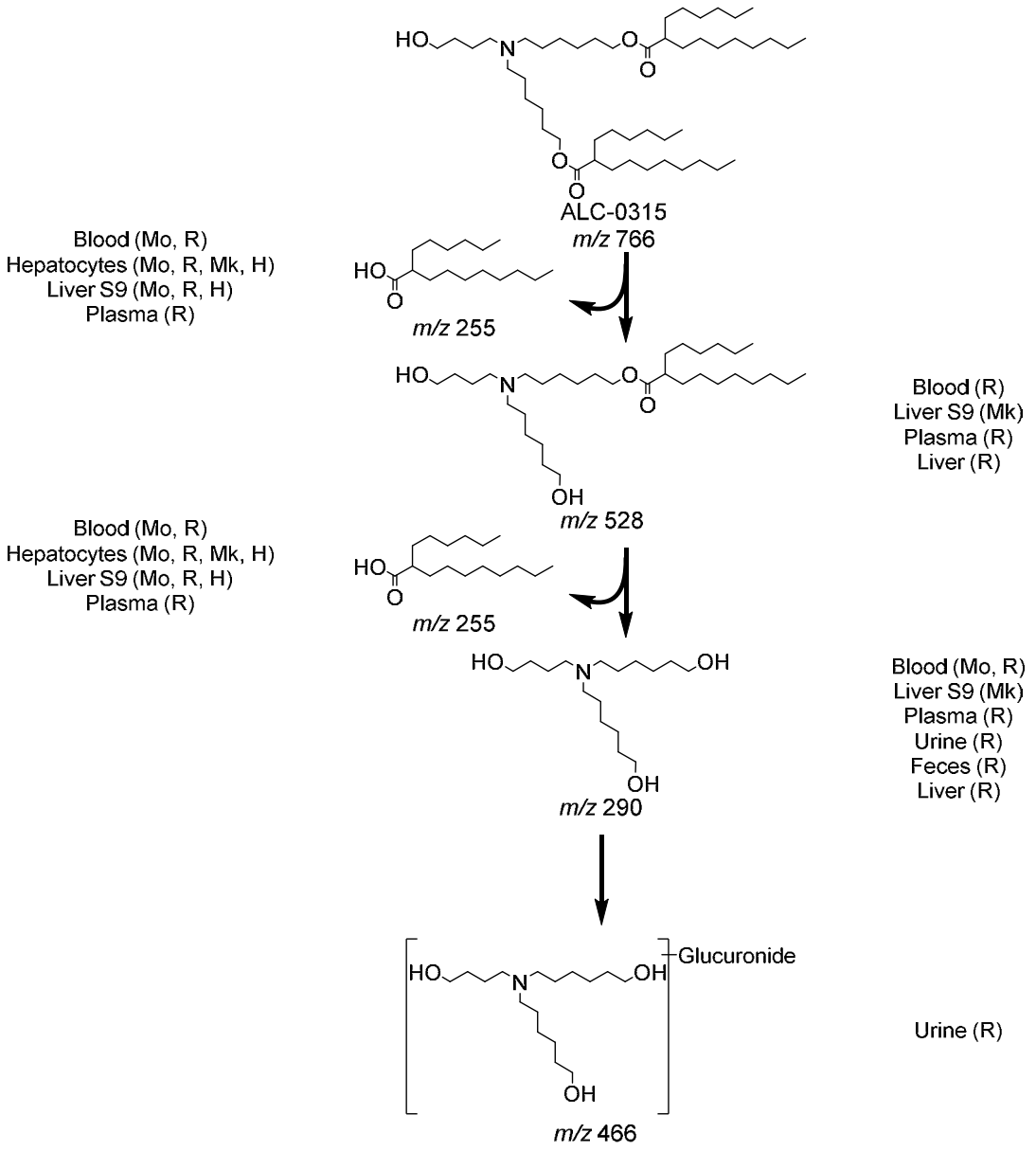

9.3. UHPLC-MS Chromatograms of Standards (A), Blank Mouse Hepatocytes 0 h (B), Blank Mouse Hepatocytes 4 h (C), ALC-0159 in Mouse Hepatocytes 0 h (D) and ALC-0159 in Mouse Hepatocytes 4 h (E)

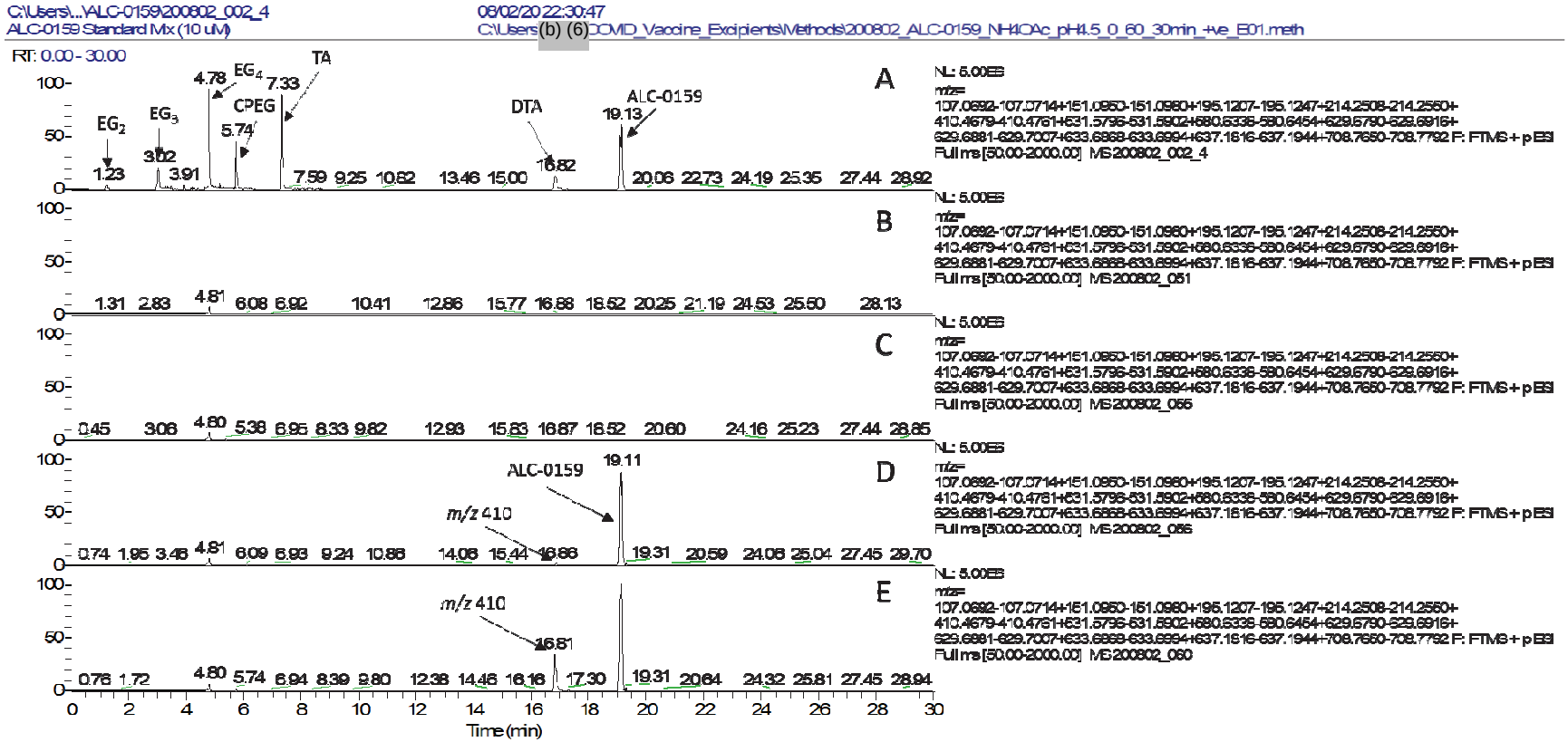

EG_2 – Diethylene glycol
EG_3 – Triethylene glycol
EG_4 – Tetraethylene glycol
CPEG – Carboxy-MPEG2
TA – Tetradecylamine
DTA – *N,N*-Ditetradecylamine

9.4. UHPLC-MS Chromatogram of Standards (A), Blank Human Hepatocytes 0 h (B), Blank Human Hepatocytes 4 h (C), ALC-0159 in Human Hepatocytes 0 h (D) and ALC-0159 in Human Hepatocytes 4 h (E)

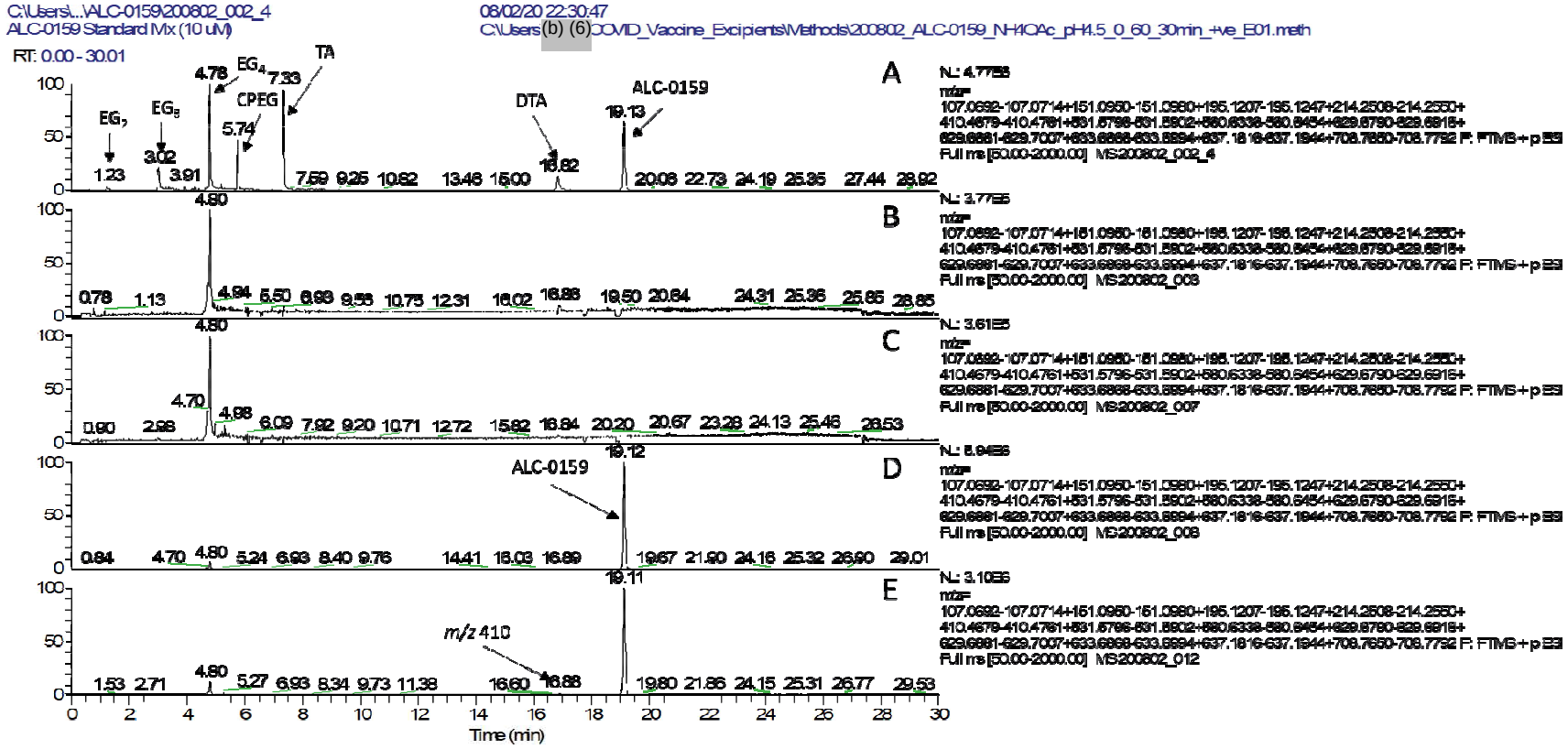

EG_2 – Diethylene glycol
EG_3 – Triethylene glycol
EG_4 – Tetraethylene glycol
CPEG – Carboxy-MPEG2
TA – Tetradecylamine
DTA – *N,N*-Ditetradecylamine

9.5. UHPLC-MS Chromatogram Standards (A), ALC-0159 in Plasma (B), Urine (C), Feces (D) and Liver (E) from a Rat Pharmacokinetics Study

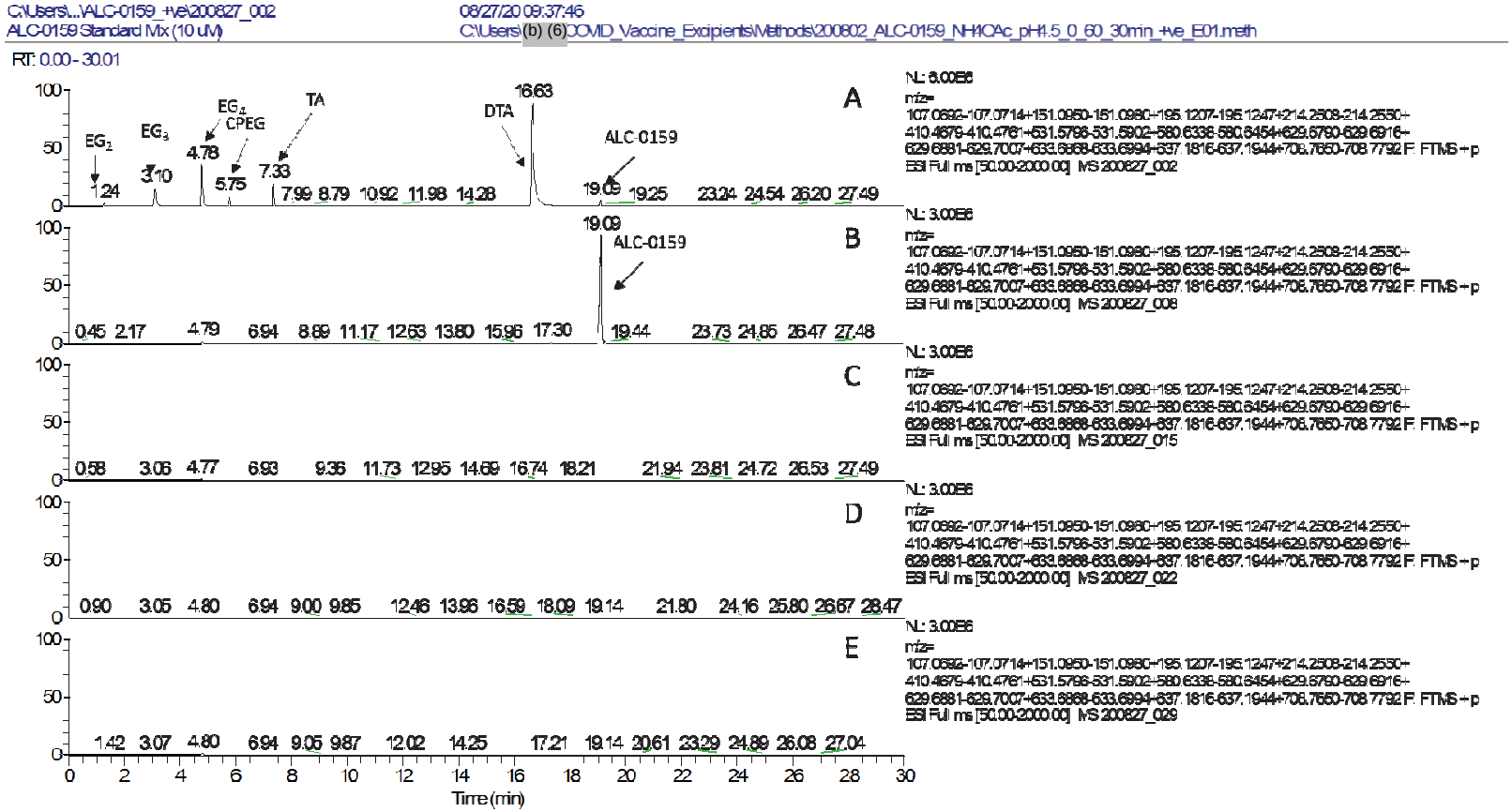

EG_2 – Diethylene glycol
EG_3 – Triethylene glycol
EG_4 – Tetraethylene glycol
CPEG – Carboxy-MPEG2
TA – Tetradecylamine
DTA – *N,N*-Ditetradecylamine

9.6. UHPLC-MS Chromatogram Standards (A), ALC-0315 in buffer (B), ALC-0315 + Monkey Liver S9 No Cofactors 24 h (C), ALC-0315 + Monkey Liver S9 Cofactors Mix A 24 h (D) and ALC-0315 + Monkey Liver S9 Cofactors Mix B 24 h (E)

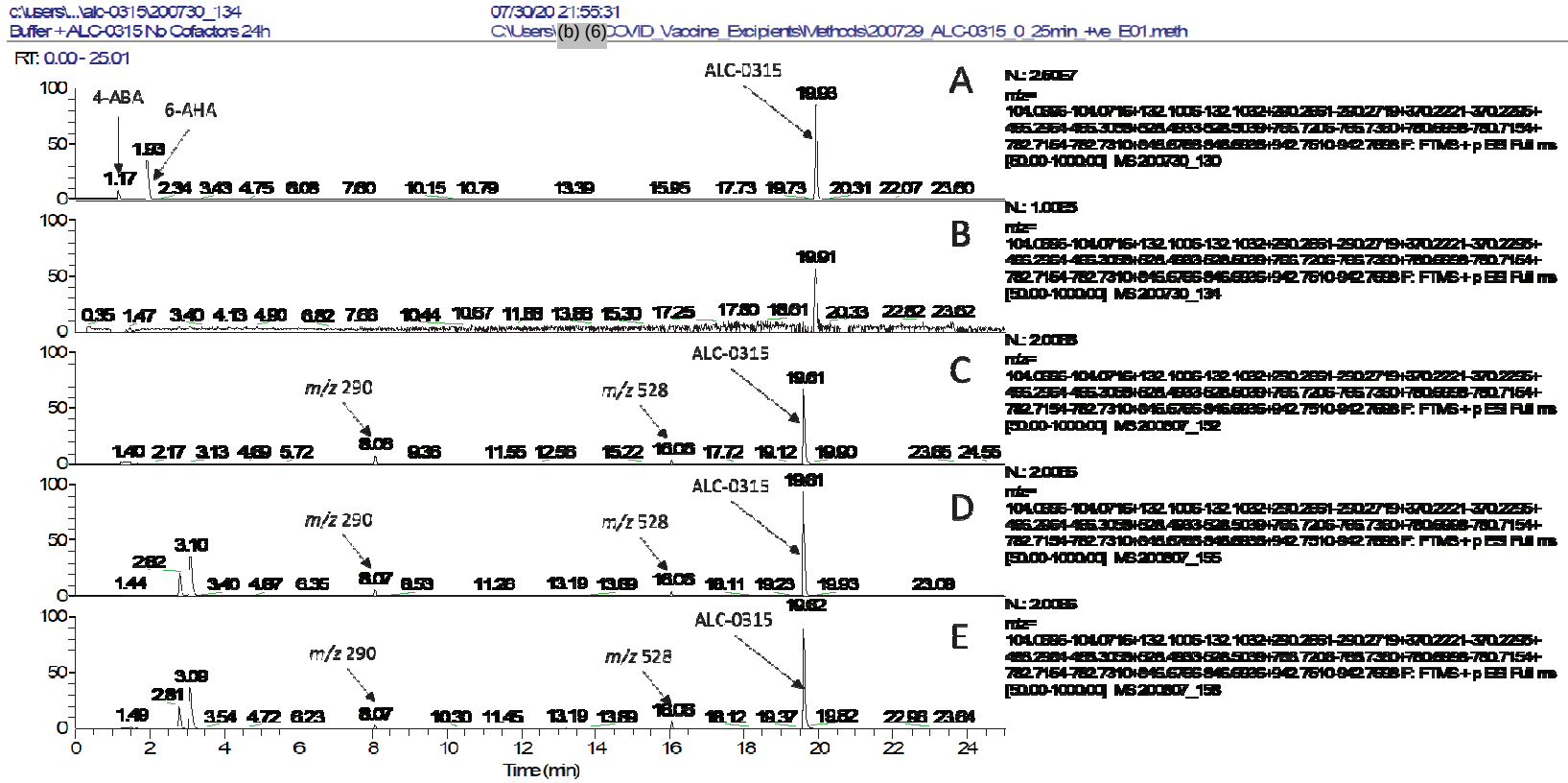

4-ABA – 4-Aminobutyric acid
6-AHA – 6-Aminohexanoic acid

9.7. UHPLC-MS Chromatogram Standards (A), Blank Human Hepatocytes 0 h (B), Blank Human Hepatocytes 4 h (C), ALC-0315 in Human Hepatocytes 0 h (D) and ALC-0315 in Human Hepatocytes 4 h (E)

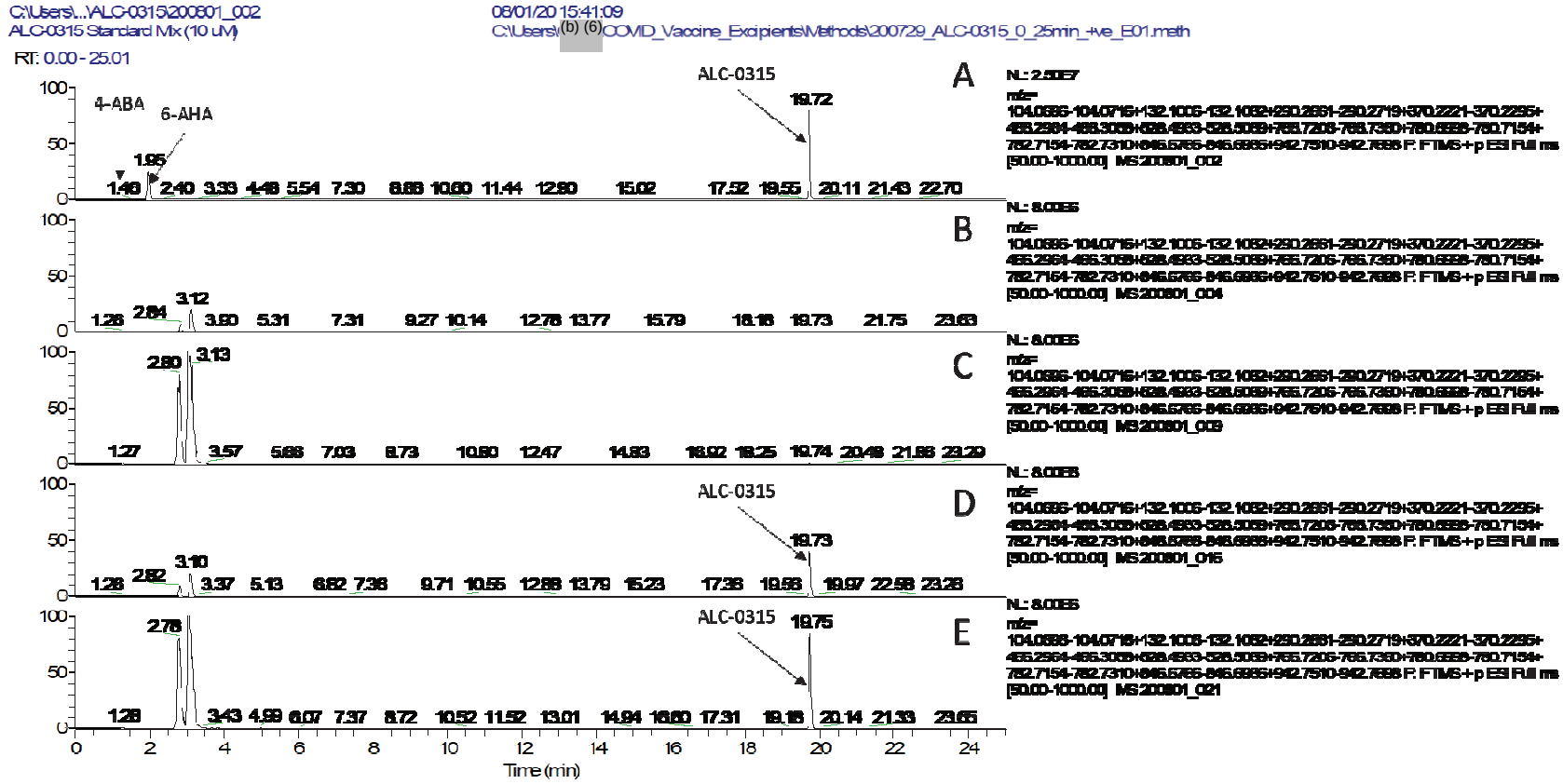

4-ABA – 4-Aminobutyric acid
6-AHA – 6-Aminohexanoic acid

9.8. UHPLC-MS Chromatogram for Standards (A), ALC-0159 in Plasma (B), Urine (C), Feces (D) and Liver (E) from a Rat Pharmacokinetics Study

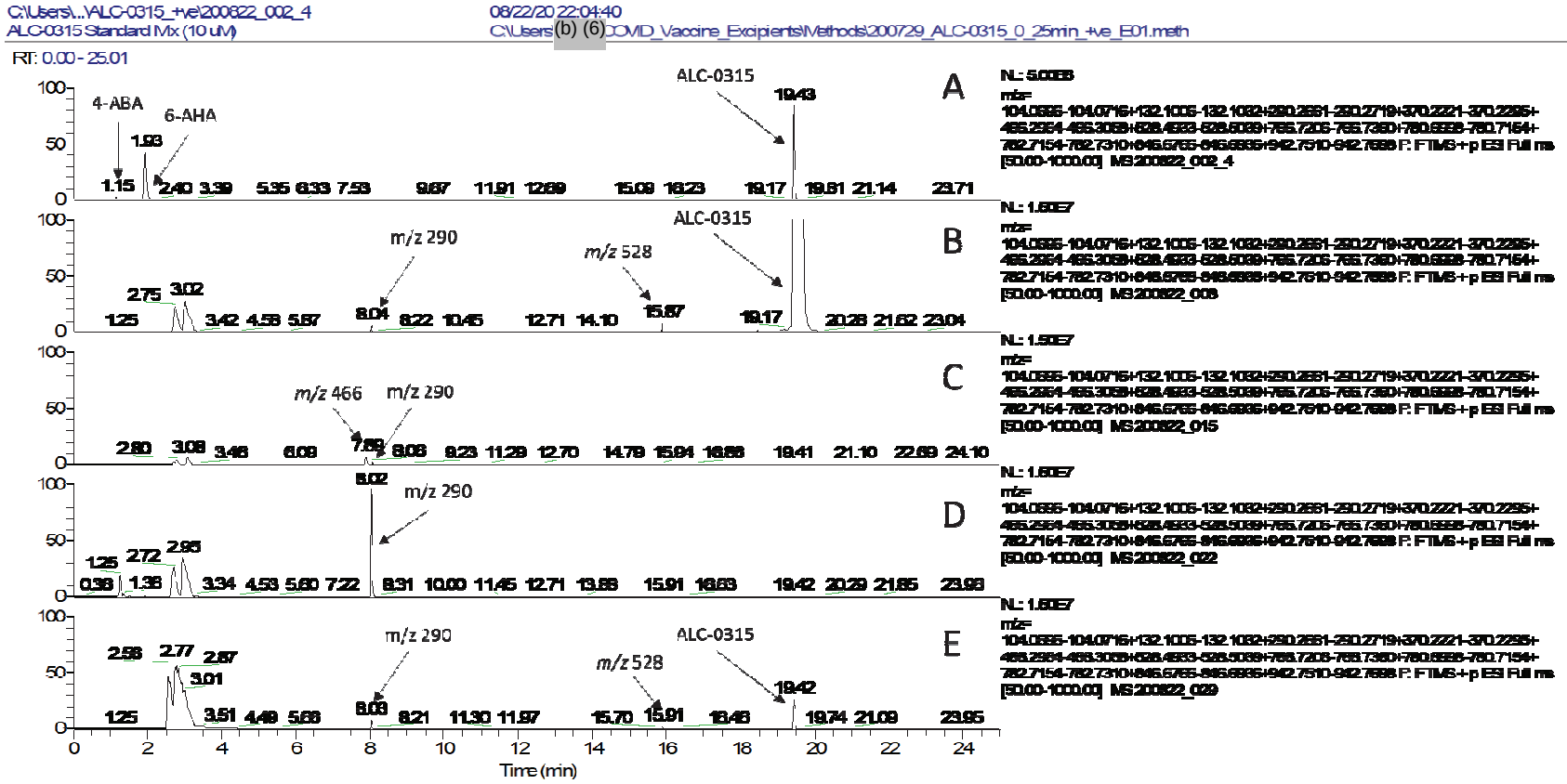

4-ABA – 4-Aminobutyric acid
6-AHA – 6-Aminohexanoic acid

9.9. Mass Spectra for ALC-0159

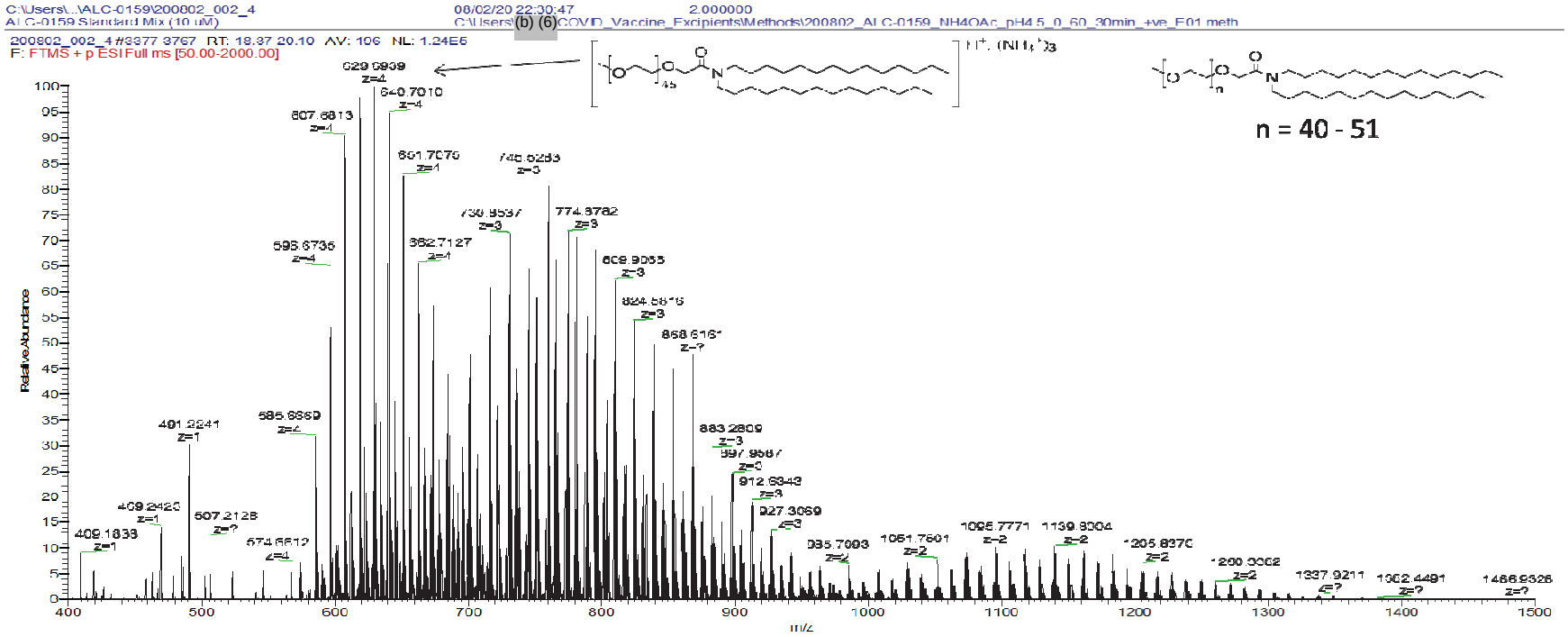

9.10. Mass Spectrum for *N,N*-Ditetradecylamine Reference Standard MS^2 (top) and ALC-0159 *m/z* 410 Metabolite MS^2 (bottom) from Incubation of ALC-0159 with Mouse Hepatocytes

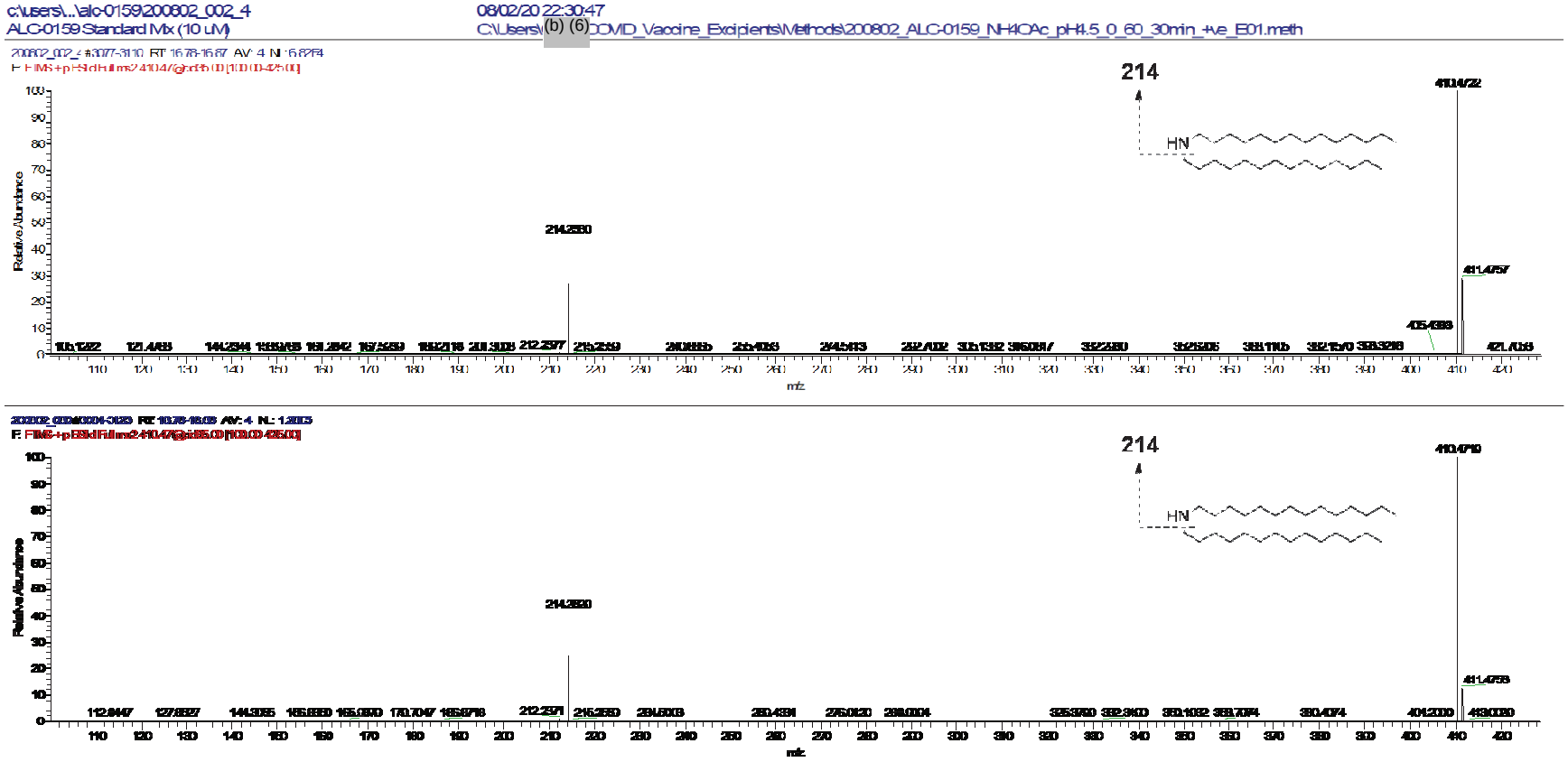

9.11. Mass Spectrum for ALC-0315 *m/z* 766 MS^2

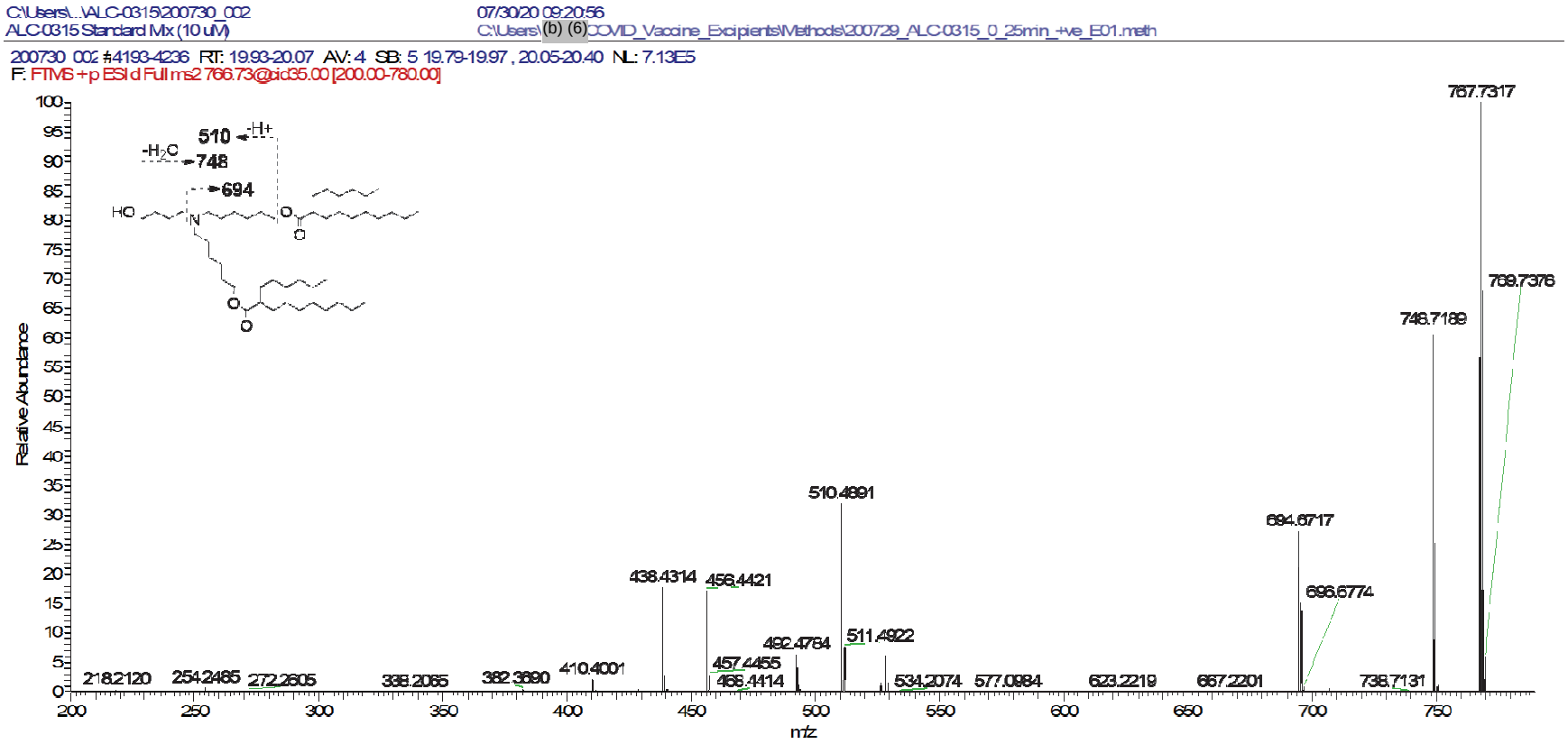

9.12. Mass Spectrum for ALC-0315 *m/z* 528 Metabolite MS^2 in Plasma from a Rat Pharmacokinetics Study

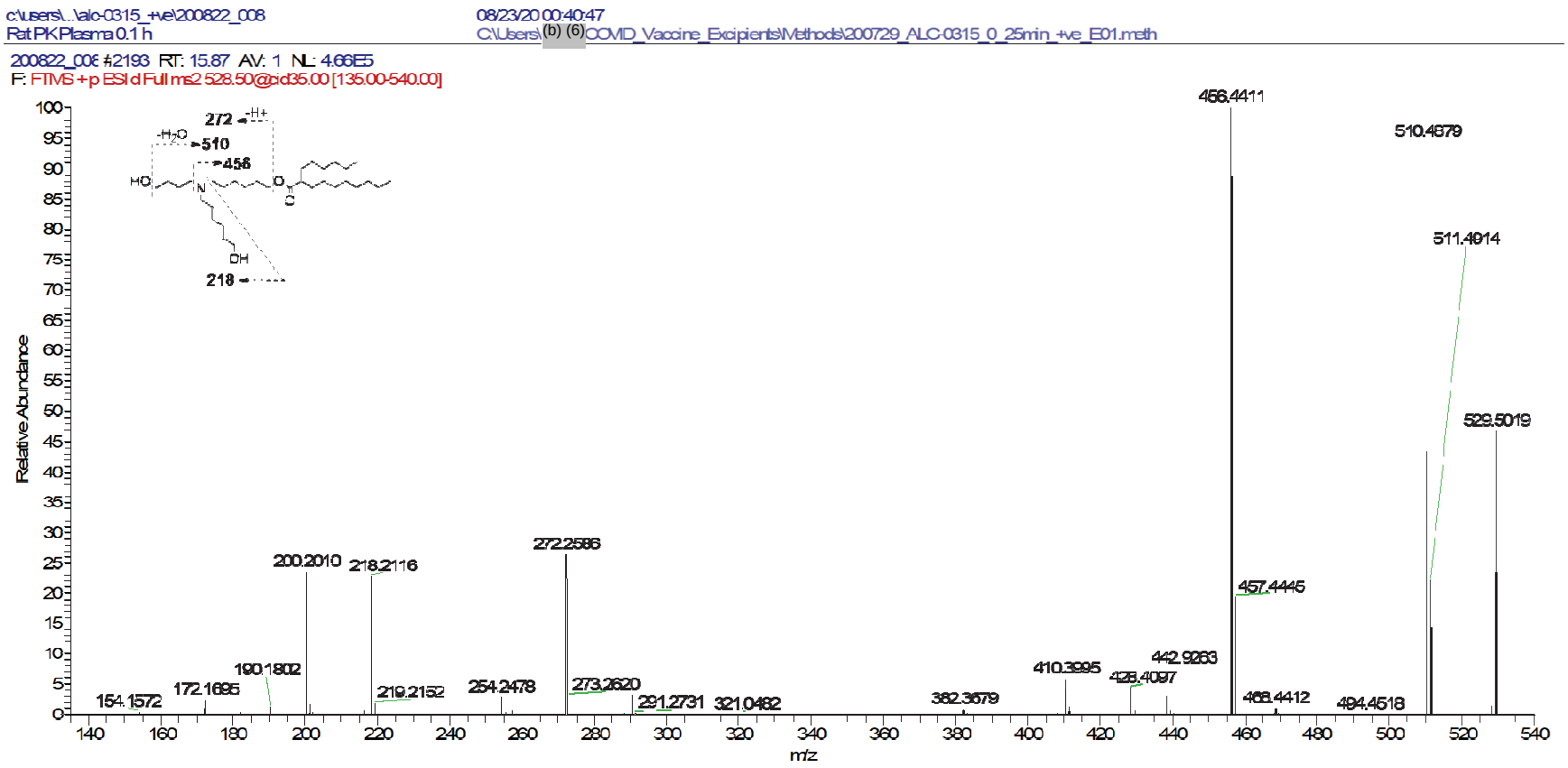

9.13. Mass Spectrum for ALC-0315 *m/z* 290 Metabolite MS^2 in Feces from a Rat Pharmacokinetics Study

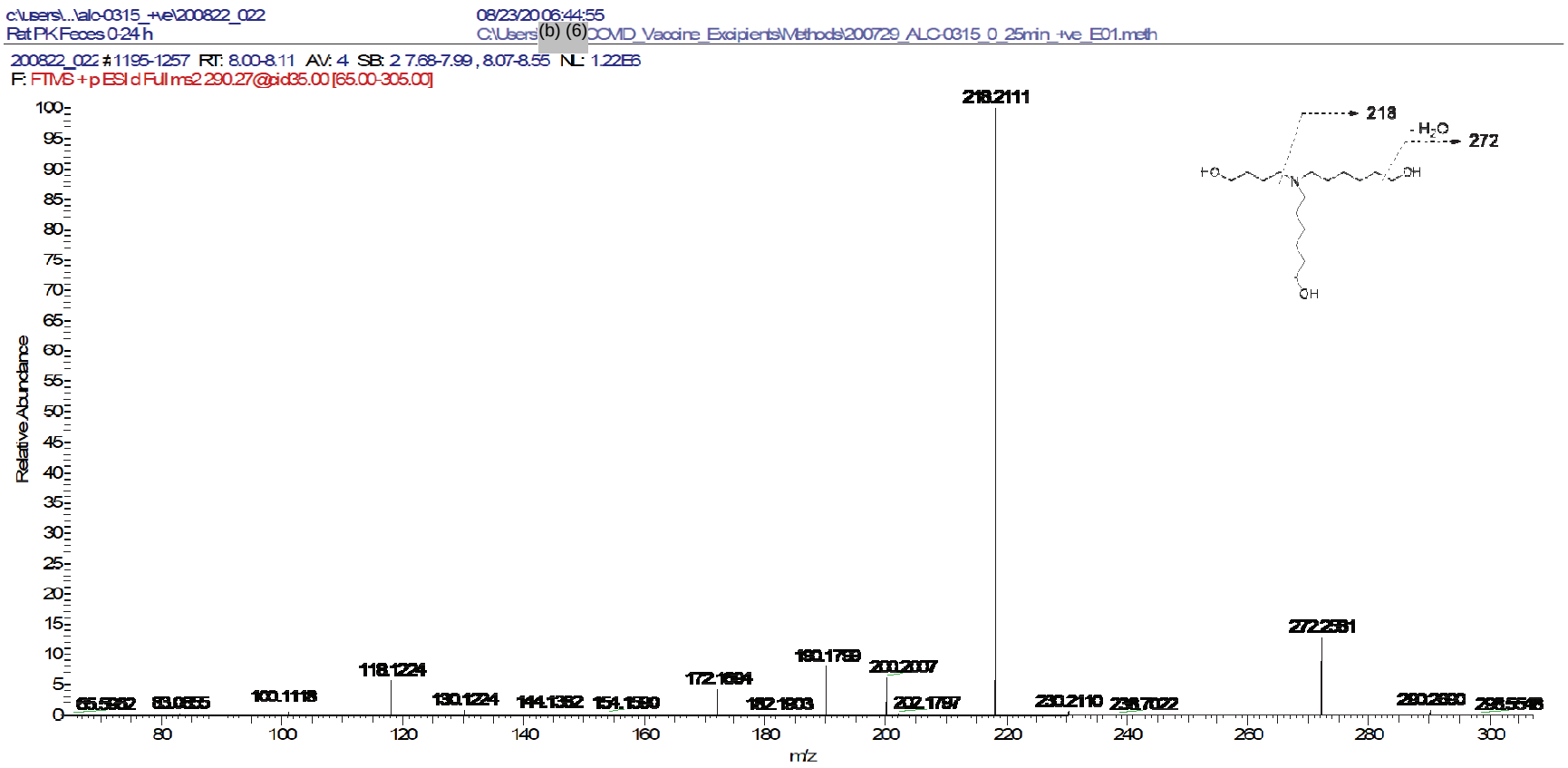

9.14. Mass Spectrum for ALC-0315 *m/z* 466 Metabolite MS^2 in Urine from a Rat Pharmacokinetics Study

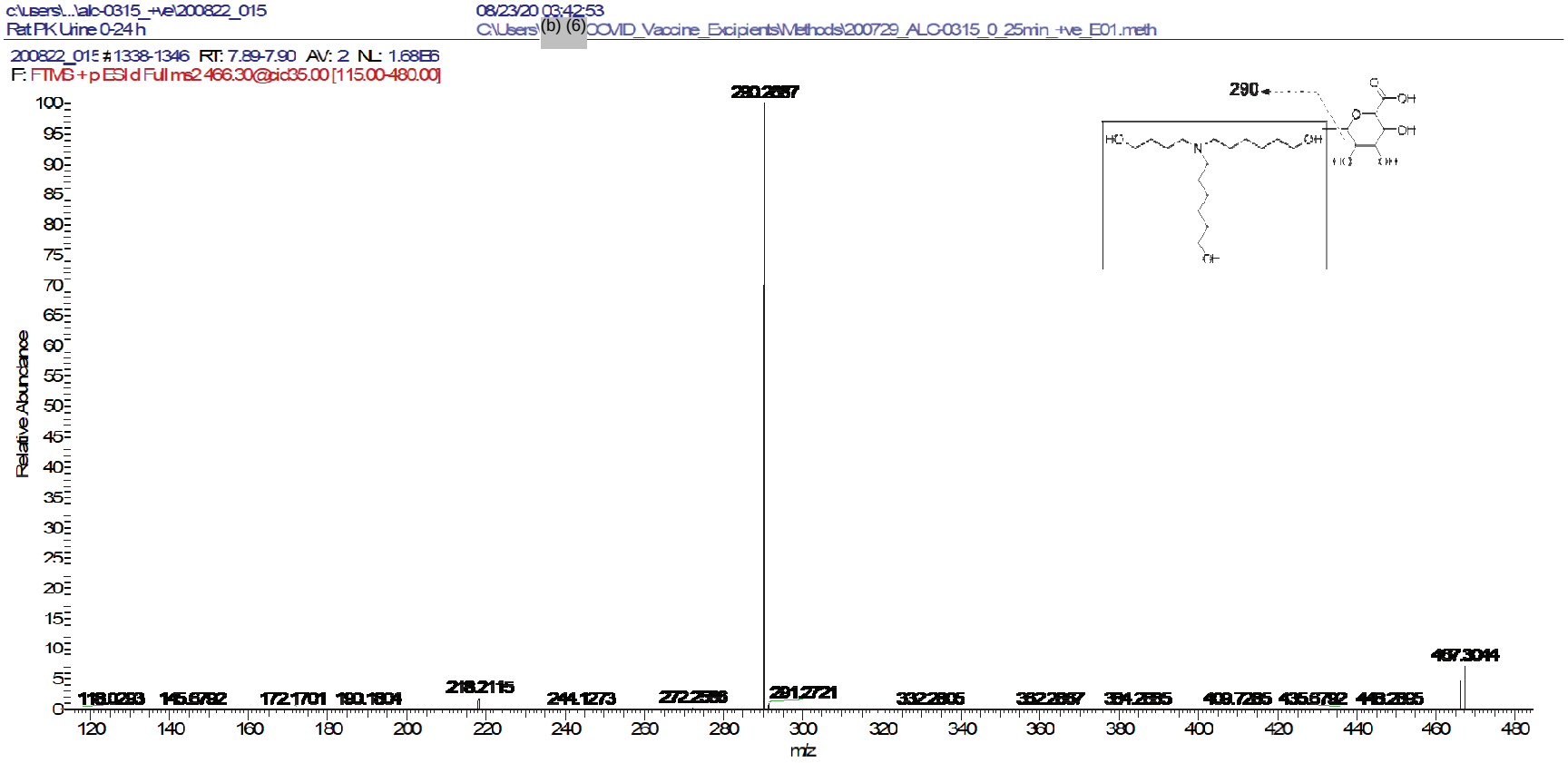

10. CONTRIBUTING SCIENTISTS

The following scientists were involved in the conduct of this study, and are responsible for the scientific content of this research report.

Contributing ADME Scientist (b) (6)

11. APPROVAL

The author and approver are responsible for the accurate representation of the data in this research report.

(b) (6)
Report Author
Pharmacokinetics, Dynamics and Metabolism, Pfizer, Groton, CT, USA

(b) (6) .
Report Approver
Pharmacokinetics, Dynamics and Metabolism, Pfizer, Groton, CT, USA

Document Approval Record

Document Name:	PF-07302048_05Aug20_043725_Investigation of the Biotransformation of ALC-0159 and ALC-0315 In Vitro and In Vivo in Rats
Document Title:	PF-07302048_05Aug20_043725_Investigation of the Biotransformation of ALC-0159 and ALC-0315 In Vitro and In Vivo in Rats

Signed By:	Date(GMT)	Signing Capacity
(b) (6)	11-Sep-2020 15:33:13	Manager Approval
	11-Sep-2020 18:13:55	Author Approval